ELSEVIER

International Journal of Adhesion & Adhesives 22 (2002) 375–384

International Journal of Adhesion & Adhesives

www.elsevier.com/locate/ijadhadh

Curing monitoring of phenolic resol resins via atomic force microscope and contact angle

Young-Kyu Lee[a], Hyun-Joong Kim[a,*], Miriam Rafailovich[b], Jonathan Sokolov[b]

[a] *Laboratory of Adhesion Science and Bio-Composites, School of Biological Resources and Materials Engineering, Seoul National University, Suwon 441-744, South Korea*

[b] *Department of Materials Science and Engineering, State University of New York at Stony Brook, New York 11794-2275, USA*

Accepted 22 May 2002

Dedicated to Professor Won-Jei Cho on the occasion of his retirement

Abstract

An atomic force microscope was used to investigate Si_3N_4 tip interactions with various curing conditions in three different molar ratios. Also the surface free energy and acid–base character of resol resin were investigated using contact angle analysis. The adhesion force between tip and surface can be calculated from the deflection distance of cantilever and the cantilever spring constant. The acid–base property of surface was characterized by calculating the work of acid–base interaction according to Fowkes' and Good's theory. And then, the adhesion force was compared to surface free energy.

The result was that the hydrophobic effect also plays a significant role in adhesion force. At the same curing temperature the adhesion force for the more hydrophobic $F/P = 2.5$ resol resin was comparatively lower than hydrophilic $F/P = 1.3$ and 1.9 resin.

Keywords: A. Phenolic; C. Atomic force microscopy; C. Contact angle; D. Cure/hardening

1. Introduction

Phenol–formaldehyde thermosetting resins have many industrial applications. Phenolic resins have been used extensively in the production of molded plastics, wood products and aerospace components. In constructing aerospace components, the most important use of phenolic resins is in the manufacturing of high-performance composites.

The chemistry of prepolymers such as resol has been very well studied in the past decades by conventional analytical techniques. The development of resins demands information of the effects of the condensation conditions on the resin structure and properties. ^{13}C-NMR spectroscopy is a useful and informative method to analyze detailed structures of phenol–formaldehyde resins. Especially, quantitative NMR analysis gives valuable information in addition to other analytical methods, for example, gel permeation chromatography (GPC), differential scanning calorimetry (DSC) and IR spectroscopy.

This study for phenol–formaldehyde resin was curing monitoring by atomic force microscopy (AFM) and contact angle.

The AFM has been developed as a powerful tool for observing surface morphology on an atomic scale [1,2]. It also provides the force curve plot which can measure the interaction between a cantilever and a sample surface as adhesive force [3,4]. Some investigators have recently used the force curve plot to measure the specific interaction between biomolecules and their complementary molecules [5–9] and the interaction between a tip coated with chemical functional groups and a sample [10,11]. Those reports have shown that the adhesive force depends on the surface materials and the adhesive force could be applied to the identification of surface materials. For qualitative and quantitative measurements of the differences in such adhesive forces, it is necessary to successively measure adhesive forces of both the sample of interest and a reference surface while keeping the cantilever at a constant condition because

*Corresponding author.
E-mail address: hjokim@snu.ac.kr (H.-J. Kim).

0143-7496/02/$ - see front matter
PII: S0143-7496(02)00017-9

the adhesive force depends on the shape of the tip, the radius of the tip curvature, contaminants and environments during the measurements. Successive measurements under a constant condition can be done by force mapping on a single sample which has different kinds of surfaces. Because the force curves in force mapping measurements are measured while the cantilever is scanning the surface laterally, the differences in the adhesive forces can be clearly related to the lateral distribution of the sample materials. The use of this technique has shown that the adhesive force between the cantilever and the surface depends on the surface morphology [12–14] and the materials [15,16].

Force curves obtained by AFM are force–distance plots measured by monitoring the deflection of a cantilever as the cantilever tip approaches or retracts from a sample. Force curves include various informations about tip–sample interaction—both physical and chemical surface properties of the sample surface, including adhesion force curves. These properties are extracted from force curves obtained at various locations and then they can map to study their distribution over the sample surface. This application note describes the measurement and construction of force curves and some of the important applications for this new technology.

Contact angle measurements have been widely used to determine physicochemical properties of solid surfaces. Indeed, these measurements can be employed to monitor the surface properties of polymers, for example, degree of wetting, critical surface tension, dispersive and polar surface free energies, acid–based surface interactions, surface crystallinity, surface orientation of functional group, surface roughness and surface contamination [17–19].

In this paper, we report on the changes in the adhesion force using AFM. Also, the measurement of the contact angles of pure liquid, with known surface tension and hence surface tension parameters, on a given solid surface determined the surface energy of resin with different molar ratios of formaldehyde/phenol.

Also, the adhesion force measurement is consistent with contact angle observations and can be related to the surface energy increase F/P molar ratio.

2. Experimental

2.1. Synthesis of resol resins

The resin syntheses were carried out in a laboratory glass reactor equipped with a stirrer, thermometer and reflux condenser, as shown in Fig. 1. The mixture of phenol and 37% aqueous formaldehyde was heated up to a temperature of 45°C and then the catalyst, 10% sodium hydroxide solution, was added. After heating the components to 90°C for 30 min and then at 90°C heating continued for 60 min. Formaldehyde/phenol (F/P) molar ratios of 1.3, 1.9 and 2.5 were prepared of solid content 55%. The fundamental properties of resol resin are listed in Table 1.

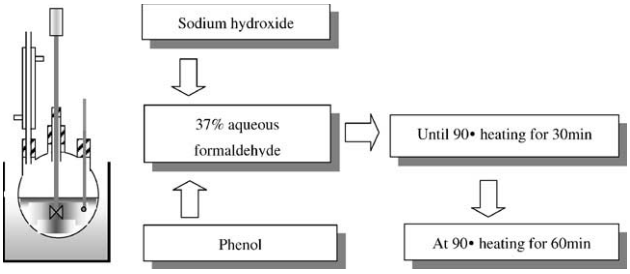

Fig. 1. Apparatus used in the preparation of resol resin.

Table 1
Characteristics of the resins

Code	Resol		
	1	2	3
F/P molar ratio	1.3	1.9	2.5
M_n	240	380	400
M_w	460	630	670
M_n/M_w	1.92	1.66	1.67
Non-volatile content (%)	59.2	53.5	50.4
Viscosity (mPa s)	157	445	1390

2.2. Adhesion force measurements

A Nanoscope III contact mode atomic force microscope (DI 3000, Digital Instruments) was used to measure the adhesion force of resol resin with various curing conditions. Nanoprobe cantilevers with silicon nitride tips were obtained from Digital Instruments. The average of the spring constant K was 0.58 N/m. This value was determined from the tip dimensions and Young's modulus.

To investigate curing behaviors by AFM, the thickness of resin was maintained at about 1000 ± 50 Å. The silicon wafer, which drop of resin is spin coated at 2500 rpm for 30 s, was cured on a hot plate.

In this study, the goal is to compare the level of cure at different curing temperature conditions of 140°C, 150°C and 160°C for 20, 30, 60, 90, 120, 150, 180, 300, 420, 600, 900, 1800, 2700 and 3600 s, respectively.

Data were acquired in terms of tip deflection (nm) versus piezo position (nm). Multiple curves were plotted together as tip deflection versus relative distance of separation (nm) by aligning their zero deflection regions (flat portion of the curves) and their constant

compliance regions (portion of curves where the cantilever moves with the surface).

The contact mode AFM including electronic control and software was used to record the force versus displacement curves, revealing the interaction between the surface of the sample and the tip. The principle of operation for the AFM is shown in Fig. 2.

Fig. 2 illustrates a typical force–distance curve between the tip and the sample surface [20]. As the sample extends upward approaching the tip from A to B, the tip is pulled down by the attractive force and jump-to-contact with the surface at B. As the sample continues to extend, the cantilever bends upward as the tip presses onto the surface. When the tip reaches position C, the sample retracts from the tip and the cantilever relaxes. As the sample continues to retract, the cantilever begins to vend downward (CD) due to the adhesion force, until reaching the break point (D) at which the cantilever rebounds sharply upward to A.

The adhesion force between tip and surface can be calculated from the deflection distance of cantilever and cantilever spring constant, as follows [20]:

$$F = k \times \Delta E, \tag{1}$$

where F is force (nN), k is the spring constant of cantilever, which was equal to 0.58 nN in this study, and ΔE is the deflection distance (nm), which in Fig. 2 is the vertical distance between point D and A. Also, approach and retraction speed of cantilever is 0.05 kHz.

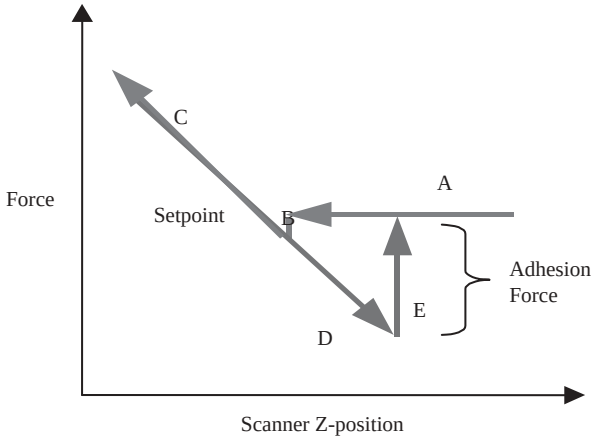

Fig. 2. A typical force–distance curve between the AFM tip and surface of sample.

The force–distance curve also provides additional information related to the elasticity of the sample surface. The cantilever deflection increases as the tip continues to press into the sample after contact, as represented by the repulsive section of BC in Fig. 2. The slope of the BC section of the force curve represents the surface elasticity.

2.3. Contact angle measurements

This study compares the level of surface free energy for curing conditions of 140°C, 150°C and 160°C for 180, 300, 420, 600, 900, 1800, 2700 and 3600 s, respectively. The coating sample cured in dry oven.

An image analysis system calculated the contour of the drop from an image captured by means of a video camera. About 15–20 measurements of the sessile drop contact angle (SEO 300A, Surface & Electro-Optics Corp.) were taken on each of three drops per liquid placed on sample. The temperature during measurements was 23 ± 1°C and the relative humidity was 55 ± 3%. In order to determine the surface free energy acid–based theory and three liquid method was used. The contact angle components of these probe liquids to be used in the studies are given in Table 2. The liquids used for surface free energy measurements were distilled water, glycerol and diiodomethane.

Three-liquid method: acid–based approach. The wetting of a solid surface by a liquid and the concept of contact angle (θ) was first formalized by Young [21]:

$$\gamma_S - \gamma_{SL} = \gamma_L \cos\theta, \tag{2}$$

where γ_L is the surface energy of liquid, γ_{SL} is the interfacial energy of solid/liquid interface and γ_S is the surface energy of solid.

This approach developed by Fowkes [17], van Oss et al. [18,19], Good [22], Good and van Oss [23] and Chaudhury [24] is the most complex one. The surface free energy is seen as the sum of a Lifshitz-van der Waals component γ_i^{LW} (corresponding to γ_i^d) and a polar, or Lewis acid–base component γ_i^{AB} (corresponding to γ_I^P). The acid–base component γ_i^{AB} can be further subdivided

Table 2
Surface energy components of probe liquids

MJ/m^2	Diiodomethane CH_2I_2	Formamide $HCONH_2$	Distilled water H_2O	Ethylene glycol $(OHCH_2)_2$	Glycerol $C_3H_8O_3$
Surface energy (γ)	50.80	58.00	72.80	47.99	64.00
Dispersive (γ^{LW})	50.80	39.00	21.80	29.00	34.00
Polar (γ^{AB})	0	19.00	51.00	18.99	30.00
Acid (γ^+)	0	2.28	25.50	1.92	3.92
Base (γ^-)	0	39.60	25.50	47.00	57.40

according to the following equation:

$$\gamma_i^{AB} = 2(\gamma_i^+ \gamma_i^-)^{1/2}, \quad (3)$$

where γ_i^+ is the electron-acceptor parameter of the acid–base surface free energy component or Lewis acid parameter of surface free energy and γ_i^- is the electron-donor parameter of the acid–base surface free energy component or Lewis base parameter of surface free energy. The mathematical approach for the solid/liquid interfacial tension is given by

$$\gamma_{SL} = \gamma_S + \gamma_L - 2(\gamma_S^{LW}\gamma_L^{LW})^{1/2} - 2[(\gamma_S^+\gamma_L^-)^{1/2} + (\gamma_S^-\gamma_L^+)]^{1/2}. \quad (4)$$

In order to determine the surface free energy components (γ_S^{LW}) and parameters γ_S^+ and γ_S^- of a solid, the contact angle of at least three liquids with known surface tension components γ_L^{LW}, γ_L^- and γ_L^-, two of which must be polar, has to be determined [17–19].

2.4. FT-IR analysis

A Perkin–Elmer Spectrum BX FTIR spectrometer at a resolution of 4 cm^{-1} was employed in the absorbance mode for resin characterization during the curing process. In order to remove moisture from the resins, the resins were mounted in the vacuum dry oven at 40°C for 48 h.

The resin was mixed with KBr (resin:KBr = 1:70) to plate and it cured in the dry oven. IR analysis is based on the fact that each chemical group in a sample absorbs IR radiation of some characteristic frequencies.

The resin mixed with KBr was cured at different curing temperature conditions (130°C, 160°C and 180°C for resol resin) for 3, 5, 7, 10, 20, and 60 min, respectively.

3. Results and discussion

3.1. Adhesion force

Contact mode AFM coated with resol resin was used to measure the adhesion force at various curing conditions.

The adhesion force curves for molar ratios of F/P are presented in Figs. 3, 4 and 5, respectively. At the same curing temperature, the adhesion force of the initial stage for $F/P = 1.3$ resin was stronger than others.

With increasing F/P molar ratio, the adhesion force is decreasing. When Figs. 3 and 5 are compared, these differences are statistically significant, and the discrepancy is reproducible in all instances.

The reason is that the increasing F/P value enhances the concentration of the methylol group. This indicates that the methylol group and other potential formaldehyde sources increases greatly with F/P molar ratio in the resol resin, and there are still some significant amounts of free ortho and para sites left. The free sites after curing clearly decrease, the higher the initial F/P ratio of the resol. At the same time, of course, the concentration of the $-CH_2O-$ unit increases. This resin has a reasonably high degree of crosslinking (i.e. from methylene bridges) as well as a significant amount of dibenzyl ether linkages and with possibly a small amount of methylol units left. This results in the increasing amount of methylene and ether bridges and further in the rigid resin structure [24].

At increasing curing time, the adhesion force is decreasing and then at the last stage it was constant. Especially, the gradual decreasing of adhesion force was shown to be invariable after about 300 s curing. This

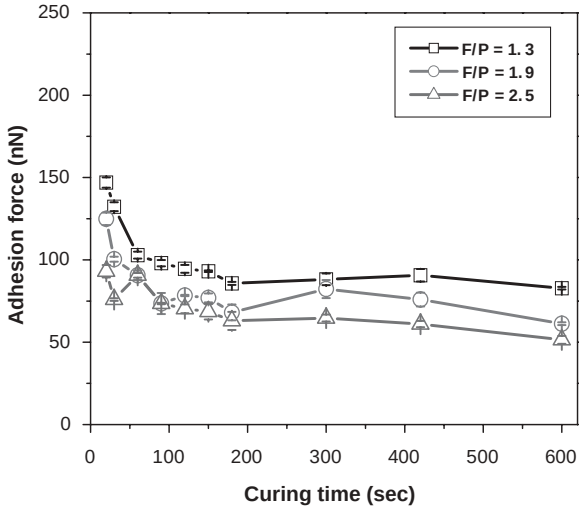

Fig. 3. AFM adhesion force curve of F/P molar ratio for curing temperature at 140°C.

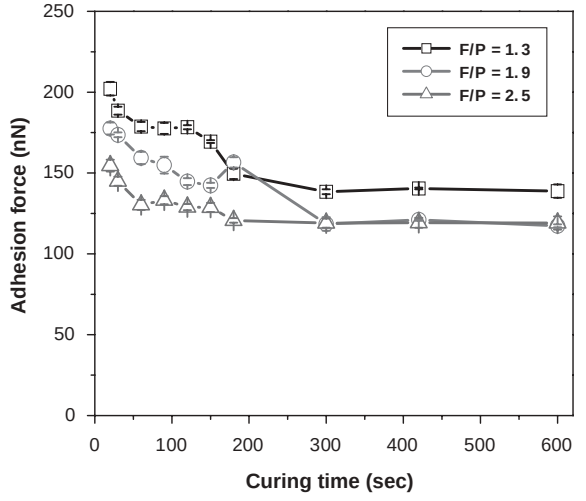

Fig. 4. AFM adhesion force curve of F/P molar ratio for curing temperature at 150°C.

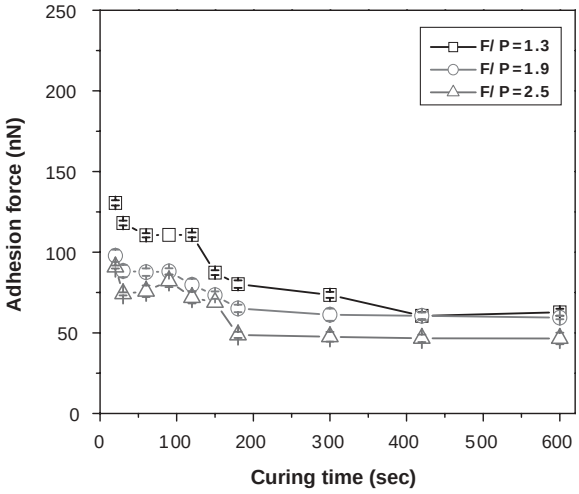

Fig. 5. AFM adhesion force curve of F/P molar ratio for curing temperature at 160°C.

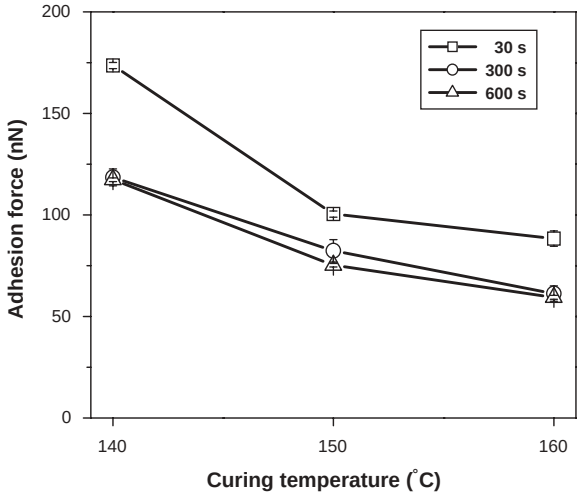

Fig. 6. AFM adhesion force curve of $F/P = 1.9$ for curing time and temperature.

suggests that all the –CH_2O– units (methylols and dibenzyl ether bridges) are eventually converted to methylene bridges. The formaldehyde that evolved during cure had likely escaped instead of condensing with phenols with free ortho and para sites [24].

The initial curing of resol resin was increased as the molar ratio of formaldehyde/phenol (F/P) increased and as the curing temperature of resins increased.

For the lower F/P molar ratio resin (i.e., 1.37), all the –CH_2O– units disappear at a curing temperature of 180°C. For the higher F/P molar ratio resin (i.e., 2.03), the –CH_2O– units essentially disappear at about 220°C.

As the curing temperature is increased the curing reaction is merely converting the –CH_2O– units onto the more thermodynamically stable methylene bridges, to reach the ultimate degree of cure [24].

Thermosetting resins exhibit individual chains that are chemically crosslinked by covalent bonds during polymerization, which give rise to a final three-dimensional network that resists heating and solvent attack but cannot be thermally processed. Resol resin is prepared by the reaction of phenol with excess formaldehyde under basic conditions. The first step in resol formation is the reaction of phenol and excess formaldehyde under basic conditions to form an addition compound followed by a condensation reaction of a methylol group in either the ortho or para position, which produces methylene bridges.

Higher F/P molar ratio promotes a higher methylol content, more polyoxy methylene oligomers and more dibenzyl ether bridges. These are all potential sources of formaldehyde in subsequent curing reactions. The effect of reaction time indicates that some of these formaldehyde sources are converted to methylene bridges with longer reaction times, to give resol with higher molecular weights.

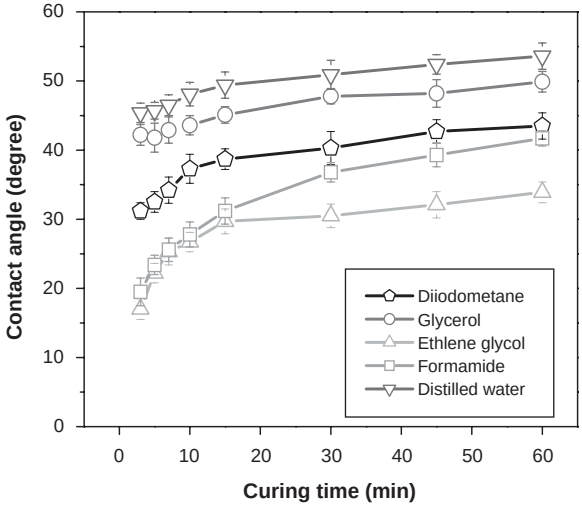

Fig. 7. Curing time-dependent contact angles for $F/P = 2.5$ at 160°C.

Fig. 6 shows the relationship between curing temperature and curing time at $F/P = 1.9$. At the curing time and curing temperature increase, the adhesion force decreases. However, for 300 and 600 s curing time, there is no real difference between the adhesion force values as the curing temperature increases.

3.2. Surface free energy

Fig. 7 expresses the contact angles of liquids with increased curing time of cured resol resin on silicone wafer. The contact angles varied with the liquids applied and this difference in wetting is governed by two factors. One is due to the adsorption of the liquid and the other is dominated by the surface acid–base interactions in agreement with the observation of Fowkes and Tischler

[25]. It is because we used liquids having different chemical properties; for example, distilled water is known with an H_2O structure and has a ratio of acid/base at 1, formamide has an $HCONH_2$ structure and a ratio of acid/base at 0.058, ethylglycol has an $(OHCH_2)_2$ structure and a ratio of acid/base at 0.041, glycerol has a $C_3H_8O_3$ structure and a ratio of acid/base at 0.068, while diiodomethane has a CH_2I_2 structure and a ratio of acid/base at zero.

3.2.1. Polar/dispersive surface energy

The polar and dispersive components of the surface energy of the resol resin were determined by using Eq. (4). The results are given in Figs. 8–11. Curing resins resulted primarily in a decrease of the polar component of surface energy. This decrease is assumed to be partially due to a decrease in the percentage of –OH functional groups but may also be dependent on the nature of the resol resin. In a previous report [26], the diminishing amount of phenolic resin OH caused the phenolic resin to polymerize each other. As shown in Fig. 16, FT-IR spectra were a high band in regions from 3600 to 3000 cm^{-1}, where the hydroxyl stretching vibration can be observed. This is attributed to the wide distribution of the hydrogen-bonded hydroxyl group, whereas a low band is observed at low curing temperature, which is the free hydroxyl group. As the temperature increased, the relative absorption of the free hydroxyl group increased while that of the hydrogen-bonded hydroxyl group decreased.

Using Eq. (4) and the obtained contact angle values, the acidity energy parameter, γ_S^+, and the associated base

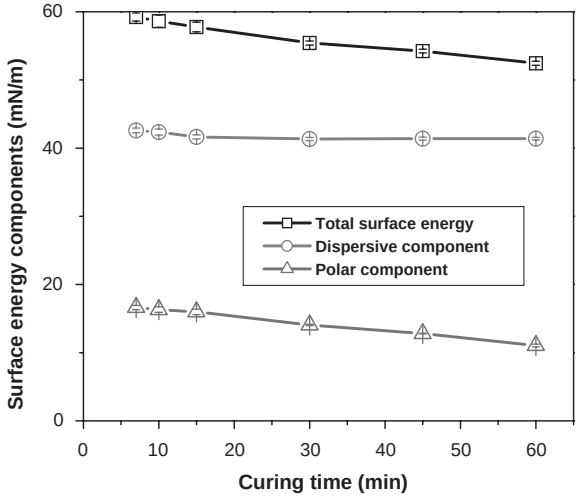

Fig. 8. Polar/dispersive components of surface energy for $F/P = 1.3$ at 140°C.

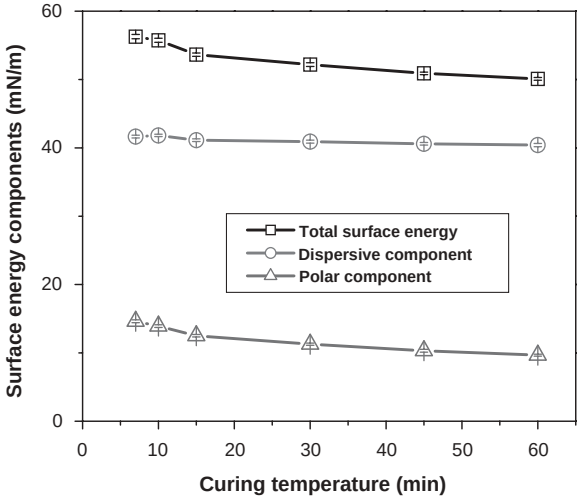

Fig. 9. Polar/dispersive components of surface energy for $F/P = 1.3$ at 160°C.

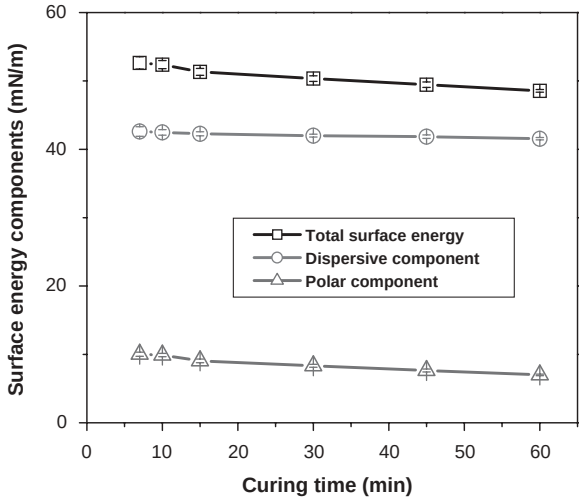

Fig. 10. Polar/dispersive components of surface energy for $F/P = 2.5$ at 140°C.

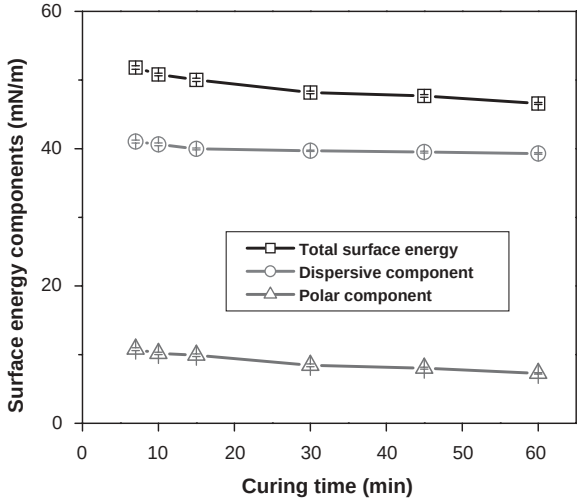

Fig. 11. Polar/dispersive components of surface energy for $F/P = 2.5$ at 160°C.

energy parameter, γ_S^-, of the specimen are determined. The specimen possesses an amphoteric property as is clearly revealed by the presence of an acid energy parameter, γ_S^+, and a base energy parameter γ_S^-. γ_S^+ and γ_S^- indicate an enhanced electron-donating ability and proton-donating ability of the wood surface, respectively. It has been found that the specimen is weaker in the electron-acceptor capability (γ_S^+) and is stronger in the electron-donor efficiency (γ_S^-) [27].

Based on our above results, we can simply express schematic models that show hydrophilic hydroxyl groups are oriented towards liquid at the resin–liquid interface, while low-energy methyl groups are exposed to the resin–air interface as shown in Fig. 15. According to this model, this surface reorientation effect has a considerable impact on the receding contact angle, since recession of water occurs on a much more hydrophilic surface than the one measured in the advancing mode, hence the considerable contact angle hysteresis observed on resin [28].

3.2.2. Analysis of acid–base components of surface energy

Because of intermolecular attractions, the molecules at the surface of a liquid are attracted inward. This creates a force in the surface, which tends to minimize the surface area. If the surface is stretched, the free energy of the system is increased. The free energy per unit surface area, or the force per unit length on the surface, is called the surface energy.

The surface free energy for resol resin curing temperature at 140°C is shown in Figs. 12 and 13. The surface free energy decreased with increasing curing temperature and molar ratio of F/P. Comparing Fig. 12 at 140°C with Fig. 14 at 160°C, the surface free energy decrease is similar to all. The increasing F/P value

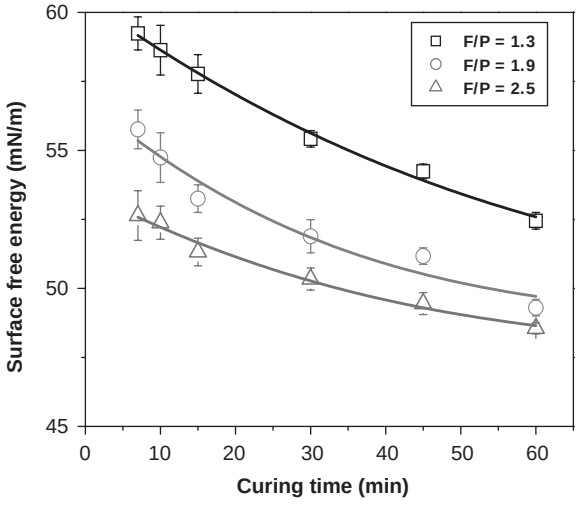

Fig. 12. Surface free energy of F/P molar ratio for curing time at 140°C.

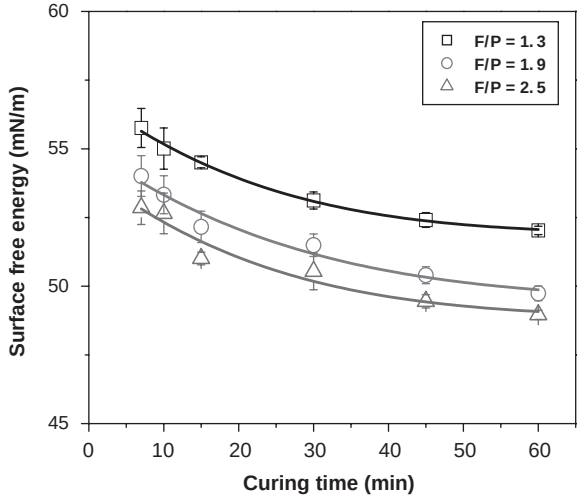

Fig. 13. Surface free energy of F/P molar ratio for curing time at 150°C.

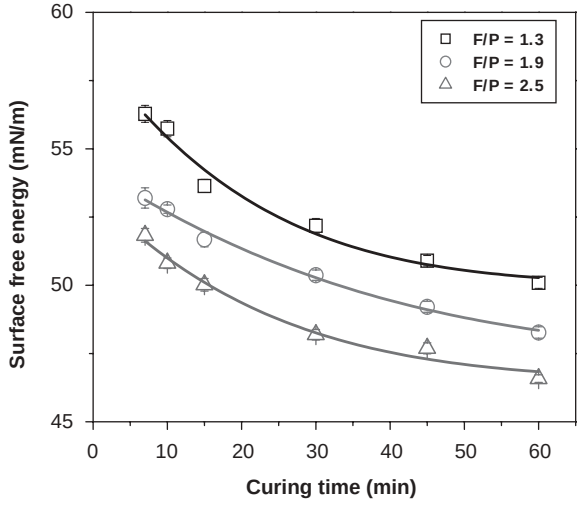

Fig. 14. Surface free energy of F/P molar ratio for curing time at 160°C.

enhances the concentration of the methylol group. This results in the increasing amount of methylene and ether bridges and further in the rigid resin structure, which makes condensation of dibenzyl ether bridges more difficult [29].

Considering that the resin surface is possibly rich in some chemical group of CH_2OH_2, it is reasonable to assume that the chemical groups present on the surface of the resin will take part in the different acid–base interactions when those chemical group liquids are penetrated. For instance, by the use of spectroscopy we find that the surface of resin is mainly rich in CH_2, while chemical groups are found to be varied in their critical surface tension.

On the basis of previous results [29–31], the amount of free ortho and para positions decrease and ortho

methylol group, $p-p'$ methylene bridges and hemiformal structures increase as a function of the increasing F/P molar ratio. The further weakening of the phenolic O–H bond is likely to lead to a stronger negative charge delocalized on the ortho and para portions of the aromatic ring. The phenol–formaldehyde self-condensation reaction is then more rapid as a consequence of the substrate-induced activation of only two types of reactive sites of phenolic oligomers.

3.3. FT-IR analysis

The principal IR absorption bands of a methylolated phenol molecule are listed in Table 3 according to the correlation described in the literatures [29,30]. The FT-IR spectra of non-cure resin are shown in Fig. 15 [26]. The deformation vibrations of the C–H bond in benzene rings give absorption bands in the 770–740 cm^{-1} range. This group disappears during the polymerization; therefore, its concentration can be used as an index of the polymerization conversion. The deformation vibration of C–C bonds in phenolic groups absorbs in the regions of 1500–1400 cm^{-1}. This group does not participate in any chemical reaction during the polymerization. However, the peak showed a gradual decrease as the polymerization processed, because when the reaction takes place, the volume of the system contracts. In particular, the absorbance at maximum of the absorption, i.e., at 740 and 1480 cm^{-1}, have been followed and scanned in the study of the reaction kinetic. The absorption peaks at 740 and 1480 cm^{-1} are named sample peak and reference peak, respectively [30].

Table 3
Methylolated phenol IR absorption bands

Functional group	Absorption	Wave number (cm^{-1})
H–O	Stretching	3330
$–CH_2$	Stretching	2900
C–C	Stretching	1612
C–C	Stretching	1598
C–C	Stretching	1480
$–CH_2–$	Bending	1450
H–O	Bending	1359
CH_2–OH	Stretching	1100

Consequently, the most important reaction involved in the alkaline polymerization of a resin is the condensation of hydroxymethyl groups with unreacted active position of other phenolic rings.

The diminishing amount of phenolic resin OH caused the phenolic resin to polymerize each other. As shown in Fig. 16 at uncured temperature, there is a high band in regions from 3600 to 3000 cm^{-1}, where the hydroxyl stretching vibration can be observed. This is attributed to the wide distribution of the hydrogen-bonded hydroxyl group, whereas a low band is observed at low curing temperature, which is the free hydroxyl group. As the temperature increased, the relative absorption of the free hydroxyl group increased while that of the hydrogen-bonded hydroxyl group decreased. This result is similar to other previous studies [30].

There are three possible condensation reaction paths for these systems, leading to the formation of a dimethylene ether of methylene chain (Fig. 17). In the first case, the mechanism involves two hydroxymethyl groups and the release of one molecule of water (Fig. 17a) with the creation of a dimethylene ether bridge. This mechanism occurs only in neutral or acid

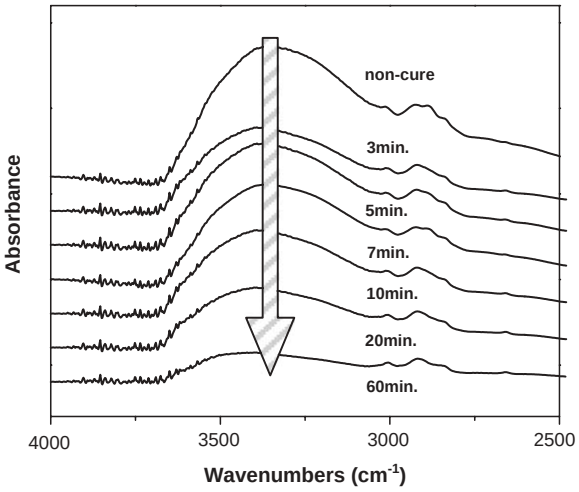

Fig. 16. FT-IR spectra for $F/P = 1.3$ at 160°C.

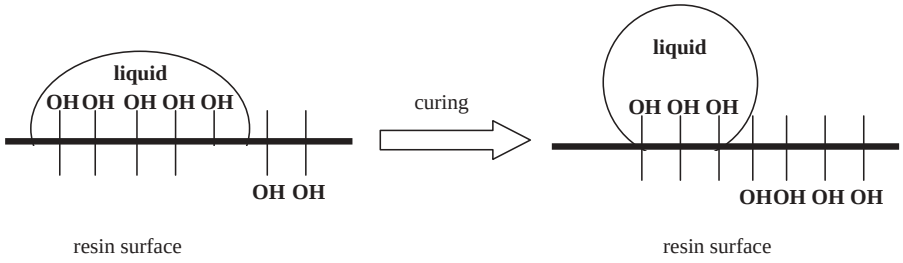

Fig. 15. Schematic models of enrichment of a surface by nonpolar components containing a polar reactive functional group.

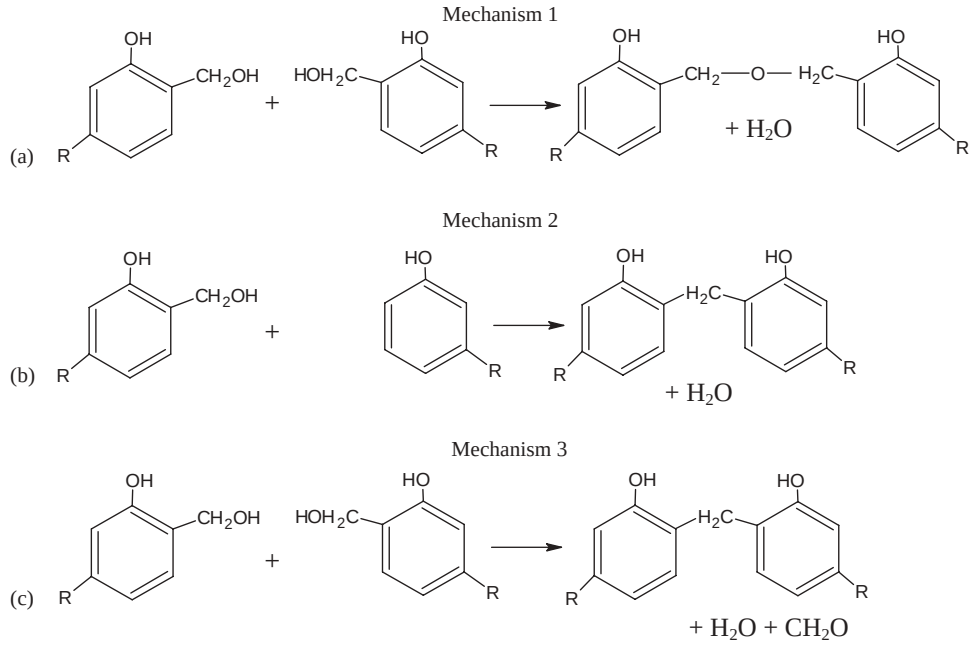

Fig. 17. Condensation reaction path of phenol–formaldehyde resin.

conditions and at temperatures less than 130°C in the case of 2,4,6-trihydroxymethylphenol, however, it is observed in the molten state starting at 80°C. The other two mechanisms involve a hydroxymethyl group with either a proton of the aromatic ring (ortho or para), with the release of one molecule of water (Fig. 17b), or a hydroxymethyl group with the simultaneous release of one molecule of water and one molecule of formaldehyde (Fig. 17c). In both cases, a methylene bridge is created [29].

4. Conclusion

Force measurements on a variety of curing time, curing temperature and F/P molar ratio show that the completely cured adhesive will have a rigid surface and easily move the tip of the AFM on an adhesive surface. The sample with a less cured adhesive is soft (viscose state) and it is difficult to move the tip of the AFM on adhesive surfaces. The magnitude of the pull-off force gives the tackiness of the resin sample and indicates how well the resin was baked and crosslinked we call it "nano tack", depending on curing conditions.

According to contact angle, surface free energies express a stronger net negative surface charge to their environment and are considered to be relatively more hydrophobic. Because the uncured resin is more hydrophobic, it appears that increasing substrate hydrophobicity results in stronger adhesion force.

The hydrophobic effect also plays a significant role in adhesion force. At the same curing temperature the adhesion force for the more hydrophobic $F/P = 2.5$ resol resin was lower than comparatively hydrophilic $F/P = 1.3$ and 1.9 resin.

Acknowledgements

This work was supported by Korea Research Foundation Grant (KRF-2000-G00078) and the NSF-MRSEC Program.

References

[1] Binnig G, Quate CF, Gerber Ch. Phys Rev Lett 1986;56:930.
[2] Sarid D, Elings V. J Vac Sci Technol 1991;9:431.
[3] Weisenhorn AL, Hansma PK, Albrecht TR, Quate CF. Appl Phys Lett 1989;54:2651.
[4] Weisenhorn AL, Maivald P, Butt H-J, Hansma PK. Phys Rev B 1992;45:11226.
[5] Moy VT, Florin EL, Gaub HE. Science 1994;266:257.
[6] Lee GU, Chrisey LA, Colton RJ. Science 1994;266:771.
[7] Florin E-L, Moy VT, Gaub HE. Science 1994;264:415.
[8] Dammer U, Popescu O, Wagner P, Anselmetti D, GuÈ therodt H-J, Misevic GN. Science 1995;267:1173.
[9] Dammer U, Hegner M, Anselmetti D, Wagner P, Dreier M, Huber W, GuÈnteherodt H-J. Biophys J 1996;70:2437.
[10] Nakagawa T, Ogawa K, Kurumizawa T, Ozaki S. Jpn J Appl Phys 1993;32:294.
[11] Frisbie CD, Rozsnyai LF, Noy A, Wrighton MS, Lieber CM. Science 1994;265:2071.
[12] Martin Y, Williams CC, Wickramasinghe HK. J Appl Phys 1987;61:4723.
[13] Torii A, Sasaki M, Hane K, Okuma S. Sensors Actuators A 1994;44:153.

[14] Sasaki M, Hane K, Okuma S, Torii A. J Vac Sci Technol B 1995;13:350.
[15] Radmacher M, Clevel JP, Fritz M, Hansma HG, Hansma PK. Biophys J 1994;66:2159.
[16] van der Werf KO, Putman CAJ, de Grooth BG. J Appl Phys Lett 1994;65:1195.
[17] Fowkes FM. J Adhes Sci Technol 1987;1:7.
[18] van Oss CJ, Good RJ, Chaundhury MK. Langmuir 1988;4: 884.
[19] van Oss CJ, Chaundhury MK, Good RJ. Adv Colloid Interface Sci 1987;28:35.
[20] Fang HP, Chan KY, Xu L-C. J Microbiol Methods 2000;40:89.
[21] Nguyen T, Johns WE. Wood Sci Technol 1979;13:29.
[22] Good RJ. J Adhes Sci Tehnol 1992;6:1269.
[23] Good RJ, van Oss CJ. In: Schrader ME, Loeb G, editors. Modern approach of wettability: theory and applications. New York: Plenum Press, 1992 [Chapter 1].
[24] So S, Rudin A. J Appl Polym Sci 1990;41:205.
[25] Fowkes FM, Tischler DO. J Polym Sci 1984;22:547.
[26] Lee YK, Kim HJ. Adhes Interface 2001;2(3):16.
[27] Shen Q, Nylund J, Rosenholm JB. Holzforschyng 1998;52:521.
[28] Morra M, Occhiello E, Garbassi F. Contact angle, wettability and adhesion. VSP BV; 1993. p. 321.
[29] Grenier-Loustalot M-F, Larroque S, Grenier P, Bedel D. Polymer 1996;37(6):955.
[30] Gao J, Liu Y, Yang L. Polym Degrad Stab 1999;63:19.
[31] Loustalot MF, Larroque S, Grenier P, Leca JP, Bedel D. Polymer 1994;35:3046.